

INFLUENȚA RAPORTULUI Zr^{4+}/Ti^{4+} ASUPRA PROPRIETĂȚILOR COMPOZIȚIILOR $0.98Pb(Zr_{1-x}Ti_x)O_3 - 0.02La(Fe^{3+0.5}, Nb^{5+0.5})O_3$ INFLUENCE OF THE Zr^{4+}/Ti^{4+} RATIO ON THE PROPERTIES OF THE $0.98Pb(Zr_{1-x}Ti_x)O_3 - 0.02La(Fe^{3+0.5}, Nb^{5+0.5})O_3$ COMPOSITIONS

ALINA IULIA DUMITRU^{1,2}, GEORGETA VELCIU¹, DELIA PĂTROI^{1*}, JANA PINTEA¹,
TUDOR-GABRIEL DUMITRU³, ILDIKO PETER^{4*}

¹National Institute for Research & Development in Electrical Engineering ICPE-CA, 313 Splaiul Unirii, 030138, Bucharest, Romania

²University of Valahia, Str. Aleea Sinaia, nr. 13, 130004 Târgoviște, Romania

³University of Bucharest, Faculty of Physics, Str. Atomistilor, Măgurele, Romania

⁴University of Medicine, Pharmacy, Science and Technology „George Emil Palade”,

Faculty of Engineering and Information Technology Str. Nicolae Iorga nr. 1, Târgu-Mureș, 540139, Romania

In this paper, some compositions belonging to the $0.98Pb(Zr_{1-x}Ti_x)O_3 - 0.02La(Fe^{3+0.5}, Nb^{5+0.5})O_3$ system have been investigated. The considered materials have been obtained by solid state reaction technique at high temperatures (1100°C, 1150°C, 1200°C and 1250°C). Three values of x (one in tetragonal region, one in Morphotropic Phase Boundary-MPB- region and one in rhombohedral region) have been chosen for the study in the range of 0.42 - 0.58. Sintering behaviour of the ferroelectric compositions has been studied by the experimental determination of the density by the method Archimedes. These ferroelectric compositions have been investigated in terms of their structural behaviour using X-ray diffraction (XRD) analysis. The XRD results have evidenced the formation of the perovskite type structure for all the studied compositions. The influence of the Zr^{4+}/Ti^{4+} ratio correlated to the sintering temperature on the degree of incorporation of the elements in the solid solution have been studied too. All the considered ferroelectric compositions have been characterized by a high anisotropy. The PZT modified compositions reveal that the piezoelectric properties are governed by the Zr^{4+}/Ti^{4+} ratio and the sintering temperature too. For the electromechanical coupling factor (k_p) the maximum value $k_p = 0.67$ has been obtained for the composition with $x = 0.58$ and sintered at 1200°C.

În această lucrare au fost cercetate unele compoziții aparținând sistemului $0.98Pb(Zr_{1-x}Ti_x)O_3 - 0.02La(Fe^{3+0.5}, Nb^{5+0.5})O_3$. Materialele au fost obținute prin tehnica reacțiilor în stare solidă la temperatură ridicată. Au fost alese trei valori compoziționale specifice (în zona tetragonală, la limita morfotropică, respectiv în zona romboedrică), cu x între 0.42 și 0.58. Comportamentul materialelor feroelectrice la sinterizare a fost studiat prin determinarea experimentală a densității, prin metoda Arhimede și din punct de vedere structural prin analiza de difracție de raze X (DRX). Analiza DRX a pus în evidență formarea unei structuri de tip perovskit pentru toate compozițiile studiate. A fost studiată influența raportului Zr^{4+}/Ti^{4+} și a temperaturii de sinterizare asupra gradului de asimilare a elementelor în soluția solidă formată. Toate compozițiile feroelectrice studiate au prezentat un grad de anizotropie ridicat, iar compozițiile cu structura PZT modificată prezintă proprietăți piezoelectrice dependente de raportul Zr^{4+}/Ti^{4+} , dar și de temperatura de sinterizare. Valoarea maximă a factorului de cuplaj electromecanic (k_p), $k_p = 0.67$, a fost obținută pentru compoziția cu $x = 0.58$, sinterizată la temperatura de 1200°C.

Keywords: lead zirconate titanate (PZT) ceramics, ferroelectric compositions, high anisotropy, piezoelectric properties, dielectric properties

1. Introduction

Ferroelectric compositions belonging to the modified lead zirconate titanate [$Pb(Zr_{1-x}Ti_x)O_3$] system can be considered one of the most investigated materials for sensors/actuators used in different applications, like aerospace vibration control, energy harvesting, microrobotics or microelectromechanical systems, etc. [1-5]. During the time, many researchers have studied the behaviour of doped $Pb(Zr_{1-x}Ti_x)O_3$ using various techniques as reported in [6, 7]. The phase diagram of the $PbZrO_3$ - $PbTiO_3$ system has been reported by Jaffe in 1971 [8]. In this diagram the development of $Pb(Zr_{1-x}Ti_x)O_3$ compositions depends on the Zr^{4+}/Ti^{4+} ratio and temperature. For the Zr^{4+}/Ti^{4+} ratio $\sim 52/48$ the piezoelectric properties have a maximum values [8-10]. The values of the properties can be modified

by doping the $Pb(Zr_{1-x}Ti_x)O_3$ system or by changing the Zr^{4+}/Ti^{4+} ratio. The structure that characterizes the $Pb(Zr_{1-x}Ti_x)O_3$ system is a perovskite structure with the general formula ABO_3 . In this formula, according to the Goldschmidt rules, the substituted into A or/and B site in ABO_3 structure can be done if the difference between the ionic rays of the two ions is less than 15%. The doped $Pb(Zr_{1-x}Ti_x)O_3$ with different substitutions have been investigated to improve the properties for various applications [11,12].

In the $Pb(Zr_{1-x}Ti_x)O_3$ system the properties can be modified/modelled by doping with different ions in A and/or B positions [13-15].

The dielectric, piezoelectric and ferroelectric properties of $Pb(Zr_{1-x}Ti_x)O_3$ system can be modified by adding donor ions (obtaining materials with soft characteristics) or acceptor ions (obtaining materials with hard characteristics) to the

* Autor corespondent/Corresponding author,

E-mail: delia.patroi@icpe-ca.ro, ildiko.peter@umfst.ro

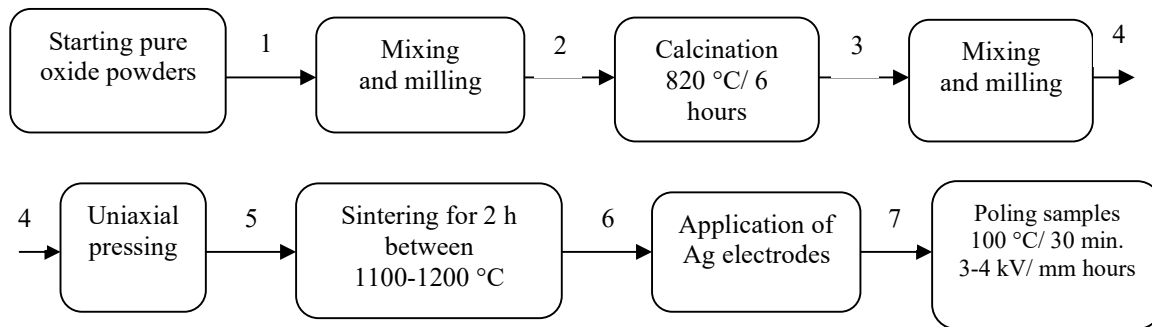


Fig. 1 - Flow chart of the mixed oxide route for obtaining new doped PZT compositions / *Diagrama pentru obținerea de noi compoziții PZT dopate prin metoda amestecării oxidilor.*

perovskite structure – of the ABO_3 type. Donor ions, like La^{3+} , Ce^{3+} , Bi^{3+} and Nb^{5+} , can be for the A site (replacing Pb^{2+}) and like Nb^{5+} and Sb^{5+} can be for the B site (replacing Zr^{4+} and Ti^{4+}) [16]. Acceptor ions like K^+ and Na^+ can be for the A site (replacing Pb^{2+}) and like Sc^{3+} and Fe^{3+} can be for the B site (replacing Zr^{4+} and Ti^{4+}) [17,18]. The effect of La^{3+} addition in $Pb(Zr_{1-x}Ti_x)O_3$ is one of the most studied effect [19]. Xiang et al. [20] have reported that the solubility limit of La in PZT is about 7.6%. According to the same authors, the tetragonality of PZT decreases as La^{3+} content increases. The Nb oxide is a very good sintering support for $Pb(Zr_{1-x}Ti_x)O_3$ systems, highlighted by Pereira et. al. [21]. Nb^{5+} can be considered as a donor dopant for $Pb(Zr_{1-x}Ti_x)O_3$ system. Nb^{5+} can substitute Pb^{2+} or (Zr^{4+} , Ti^{4+}) ions, while the solubility limit of Nb^{5+} in $Pb(Zr_{1-x}Ti_x)O_3$ system is about 7%.

Fe^{3+} substitutes (Zr^{4+} , Ti^{4+}) ions in $Pb(Zr_{1-x}Ti_x)O_3$ system and it is considered an acceptor dopant. Doping pure PZT with acceptors ions Fe^{3+} in B site creates oxygen vacancies in the lattice and doping pure PZT with donor ions such as La^{3+} (at A-site) and Nb^{5+} (at B-site) creating A-site vacancies in the lattice [22,23]. Addition of Fe_2O_3 in PZNT system influences the transition temperature to higher end and brings structural changes in the material and near MPB showing improved hysteresis loop compared to pure PZT, in agreement with the study of A. Kumar and S. K. Mishra [24].

In the present paper synthesis of ferroelectric materials, with a general formula $0.98Pb(Zr_{1-x}Ti_x)O_3 - 0.02La(Fe^{3+}_{0.5}, Nb^{5+}_{0.5})O_3$, for different Zr^{4+}/Ti^{4+} ratios have been considered and investigated. The materials have been prepared by a solid-state reaction technique.

2. Experimental Methods

Three ferroelectric compositions, described by the general formula of $0.98Pb(Zr_{1-x}Ti_x)O_3 - 0.02La(Fe^{3+}_{0.5}, Nb^{5+}_{0.5})O_3$ with x having the values of 0.58, 0.48 and 0.42 have been obtained by solid state reaction technique. These ferroelectric

compositions were obtained in Zr^{4+}/Ti^{4+} stoichiometry equals to 42/58 (PZT-I1), 52/48 (PZT-I2) and 58/42 (PZT-I3).

The flow chart has been adopted to the new compositions and the main steps of the route used to obtain the doped PZT [25] have been illustrated in Figure 1.

Polycrystalline ferroelectric materials have been obtained using PbO , TiO_2 , ZrO_2 , Fe_2O_3 , Nb_2O_3 and La_2O_3 oxides with high purity ($\geq 99\%$). The oxide powders have been mixed and ball-milled for 10 h using ethanol media. After drying, the resulting powders have been calcined 6 h at $820^\circ C$ in a closed alumina crucible under air with a PbO atmosphere. The calcined powders have been re-milled for 16 h, dried again and mixed with 5 wt% polyvinyl alcohol (PVA) solution as a binder. The powders have been pelletized under 700 kg/cm^2 pressure using a hydraulic press. The pellets (compact discs with 12 mm diameter, 1.8 mm thickness) have been sintered for 2 h in air atmosphere in a closed alumina crucible under PbO atmosphere at $1100^\circ C$, $1150^\circ C$, $1200^\circ C$ and $1250^\circ C$. Sintered pellets have been lapped until the height of 1 mm were obtained with a super water-soluble Fujimi type abrasive paste. The electrodes have been obtained by metallizing the pellets surfaces with silver paste and in the end heated to $650^\circ C$ for 30 min. before using the samples for electrical measurements. To determine the piezoelectric properties the samples have been polarized in a DC field of 3.5 kV/mm in a silicon oil bath at $100^\circ C$ for 30 min. The densities of the sintered ferroelectric compositions have been measured by Archimedes method. The crystalline structure of the sintered ferroelectric compositions has been investigated by X-ray diffractometer with $CuK\alpha$ radiation and Ni filter. The tetragonal, tetragonal-rhombohedral and rhombohedral phases have been characterized and their lattice parameters have been calculated. The morphology of the sintered ferroelectric compositions has been studied by Scanning Electron Microscopy (SEM). The P-E hysteresis loops of the un-poled samples have been measured using the TF analyser 2000. The

capacitance and the loss factor ($\tan \delta$) have been measured at 1kHz using LCR meter HM 8018. After 24 h of poling the electromechanical planar coupling factor (k_p) and electromechanical thickness coupling factor (k_t) have been determined by the resonance and anti-resonance frequency method using an impedance analyser 4294A.

3. Results and discussion

3.1. Sintering behaviour of the ferroelectric compositions

The influence of the sintering temperature on samples belonging to the three ferroelectric compositions has been studied by the experimental determination of the density employing the Archimedes method. The addition of dopants (La^{3+} , Nb^{5+} , Fe^{3+}) in $Pb(Zr_{1-x}Ti_x)O_3$ system influences the microstructure and the ferroelectric properties of the compositions [26-29]. Also the properties depend on the value of the Zr^{4+}/Ti^{4+} ratio. Thus the PZT-I1 is situated in tetragonal region (T), PZT-I2 is situated in Morphotropic Phase Boundary (MPB) region and PZT-I3 is situated in rhombohedral (RH) region.

By adding donor ions such as La^{3+} (for A^{2+} site) and Nb^{5+} (for B^{4+} site) in the $Pb(Zr_{1-x}Ti_x)O_3$ system, "soft" materials have been developed, according also to [6]. The introduction of Fe^{3+} ions as a dopant in position B^{4+} in the $Pb(Zr_{1-x}Ti_x)O_3$ system leads to oxygen vacancies, as a result the material becomes "hard". As reported in Table 1, all PZT-I1, PZT-I2 and PZT-I3 compositions sintered for 2 hours at $1100^\circ C$ demonstrate a real density situated in the range of 70.40÷73.00 % of the theoretical density, data in line with some those reported in the scientific literature [21,30]. As the sintering temperature increases to $1200^\circ C$ with a holding time of 2 hours at the final temperature, the relative density increases, reaching 92% of the theoretical density for the PZT-I2 sample. At temperatures higher than $1250^\circ C$ in all samples, it is observed that the real density drops up to 89% of the theoretical density [30]. One of the reasons that can be connected to

the reduced sample density at temperatures above $1200^\circ C$ may be caused by the PbO evaporation due to the presence of dopant ions [27]. For all sintering temperatures the best values are obtained for the PZT-I2 composition which is located in the MPB region.

3.2. Structural analysis

Figure 2 reports the XRD patterns for each sintering temperature ((a)- $1100^\circ C$, (b) - $1150^\circ C$, (c) - $1200^\circ C$ and (d) - $1250^\circ C$) for 2h of the compositions having three different Zr^{4+}/Ti^{4+} ratio of 42/58 ↔ PZT-I1, 52/48 in (MPB) region ↔ PZT-I2 and 58/42 ↔ PZT-I3 respectively. XRD results show that the studied compositions were pyrochlore phase free, and diffraction peaks match with the ICDD database card of PZT. This means that by this experimental flux the PZT with high phase purity can be obtained. The patterns were associated to a perovskite structure since no other secondary crystalline phases were identified, and further indexed by ICDD PDF file #01-072-7167 for a tetragonal crystalline structure (T), $P4mm$ (99) space group, with theoretical lattice parameters of $a=4.04 \text{ \AA}$, $c=4.13 \text{ \AA}$, and consequently with c/a ratio of 1.02. The main attributed phase suggests a homogeneous diffusion of the dopants (La^{3+} , Nb^{5+} and Fe^{3+}) into the PZT lattice to form a solid-solution, with some specific position of atoms attributed to some peak displacements with respect to the theoretical position of PZT pattern form PDF file.

Also, some observed peak splitting, i.e. $\{001\}$, $\{101\}$, $\{002\}$, and $\{112\}$ crystalline planes for PZT-I1, $\{001\}$ and $\{002\}$ crystalline planes for PZT-I2, $\{110\}$, $\{111\}$, $\{120\}$ and $\{121\}$ crystalline planes for PZT-I3, and it can be attributed to the presence of a prevalently tetragonal structure. A single PZT structure is easier to form for Ti-rich composition than for Zr-rich composition, the (002) and (200) reflections show the evidence of the coexistence also of a rhombohedral phase (R), with a higher presence in the case of Zr-rich composition.

Details of the lattice parameters have been presented in Figure 3. For the Ti-rich composition,

Table 1

Sintering behaviour of the ferroelectric compositions / *Comportamentul la sinterizare al compozițiilor feroelectrice*

T [°C]	Samples	Experimental density [g/cm ³]	Relative density [%]
1100	PZT-I1	5.77	70.40
	PZT-I2	5.99	73.00
	PZT-I3	5.88	72.00
1150	PZT-I1	5.79	70.60
	PZT-I2	7.54	92.00
	PZT-I3	7.37	90.00
1200	PZT-I1	7.48	91.30
	PZT-I2	7.52	92.00
	PZT-I3	7.38	90.00
1250	PZT-I1	7.32	89.30
	PZT-I2	7.42	91.00
	PZT-I3	7.28	89.00

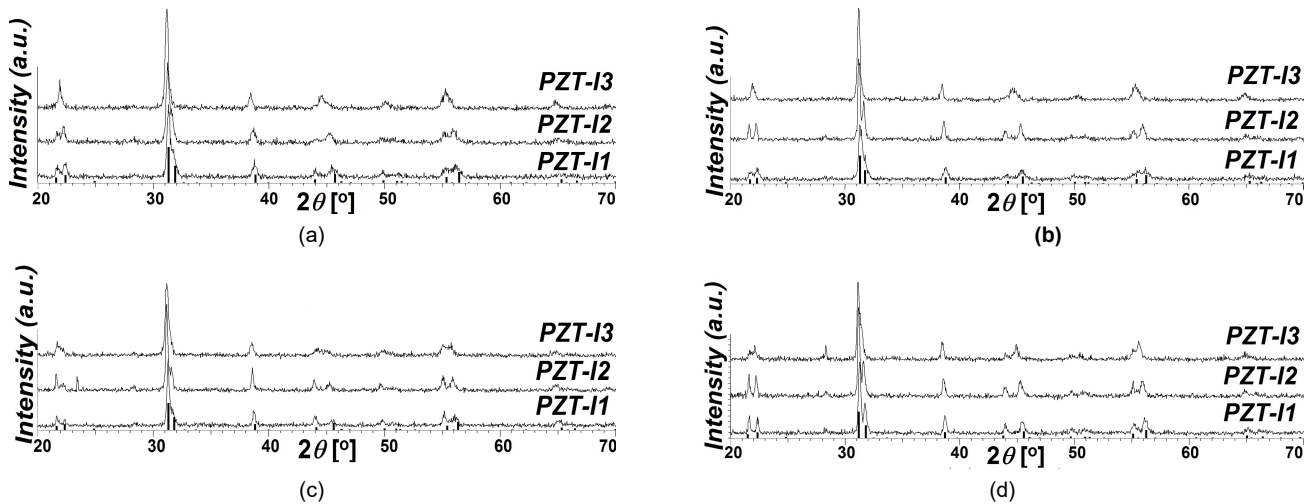


Fig. 2 - XRD patterns of PZT-I1, PZT-I2 and PZT-I3 ceramics sintered for 2h at ((a)-1100°C, (b) -1150°C, (c) -1200°C and (d) -1250°C
Diagramele DRX pentru ceramicile PZT-I1, PZT-I2 și PZT-I3 sinterizate la ((a)-1100°C, (b) -1150°C, (c) -1200°C și (d) -1250°C.

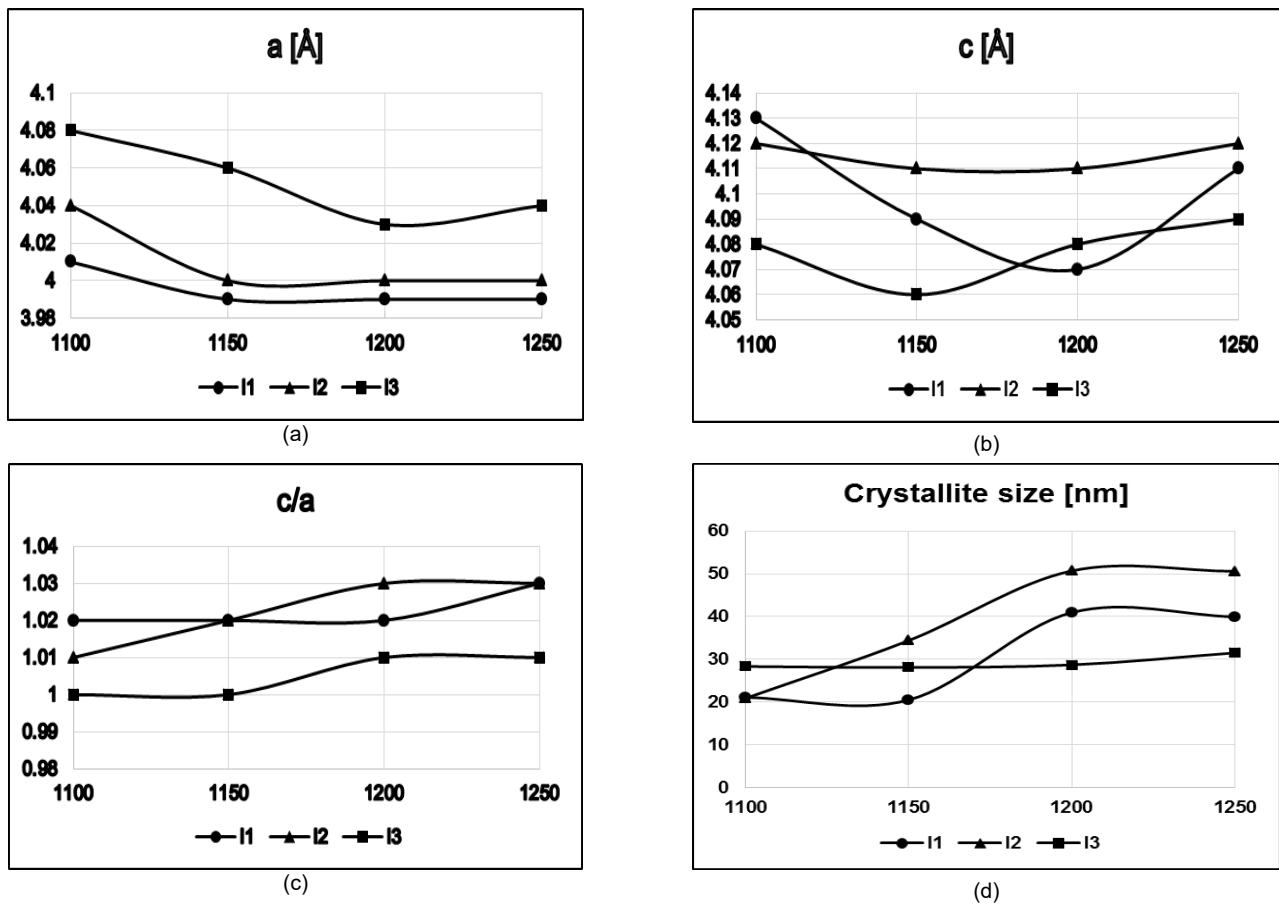


Fig. 3 - The changes in unit cell parameters and tetragonality versus composition for the sintered samples at different temperatures
Modificările parametrilor celulei elementale și ale tetragonității pentru probele sinterizate la diferite temperaturi.

lattice parameter a has an increased value with respect to the Zr-rich composition for all the sintering temperatures. In what concerns the lattice parameter c , for Ti-rich composition the minimum value is at 1200°C, with respect to the Zr-rich composition having the minimum value on the other side of the MBP composition, at 1150°C.

However, both composition regions have lower c values with respect to MBP composition for

all the sintering temperatures, which can be attributed to the specific positions of the dopants in lattice structure and different crystalline R/T ratio, contributing simultaneously to the thermodynamic behaviour of solid phase formation.

The maximum value of c/a ratio is observed at the same temperature, 1200°C, for 1.03 for MBP and 1.02 for Zr-rich composition, while Ti-rich composition is reaching the maximum value for c/a of 1.03 ratio only at 1250°C [31-33].

3.3. Ferroelectric characteristics

Figures 4-7 reports the ferroelectric hysteresis loops of all unpoled compositions (a) PZT-I1, (b) PZT-I2 and (c) PZT-I3 sintered for 2 hours at 1100°C, 1150°C, 1200°C and 1250°C at room temperature. It can be observed that all compositions sintered for 2 hours at 1100°C shows a hysteresis loops which are similar to the hysteresis loops of the conductive materials. At 1200°C and 1250°C, the compositions PZT-I1(a) and PZT-I2(b), sintered for 2 hours, shows

hysteresis loops which are similar to the hysteresis loops of the “hard” PZT ceramics. For PZT-I3(c) composition sintered for 2 hours at 1200°C and 1250°C the hysteresis loops are comparable to “soft” PZT hysteresis loops [34,35].

The direction in which the electrical coercivity and remnant polarization are changing can be explained by the motion of domain wall. The domain wall motion is influenced by the grain size of the ceramics and the type of vacancy defects [36].

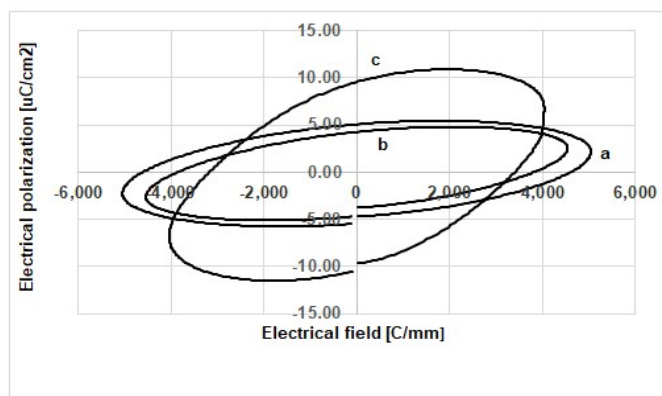


Fig.4 - Room temperature ferroelectric hysteresis loops of compositions (a) PZT-I1, (b) PZT-I2 and (c) PZT-I3 sintered for 2 h at 1100°C/ Curbele de histerezis la temperatura camerei pentru compozițiile (a) PZT-I1, (b) PZT-I2 și (c) PZT-I3 sinterizate timp de 2 ore la 1100°C.

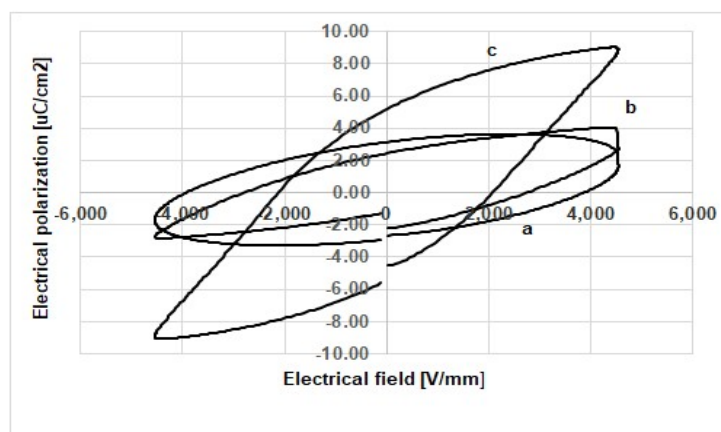


Fig.5 - Room temperature ferroelectric hysteresis loops of compositions (a) PZT-I1, (b) PZT-I2 and (c) PZT-I3 sintered for 2 h at 1150°C/ Curbele de histerezis la temperatura camerei pentru compozițiile (a) PZT-I1, (b) PZT-I2 și (c) PZT-I3 sinterizate timp de 2 ore la 1150°C.

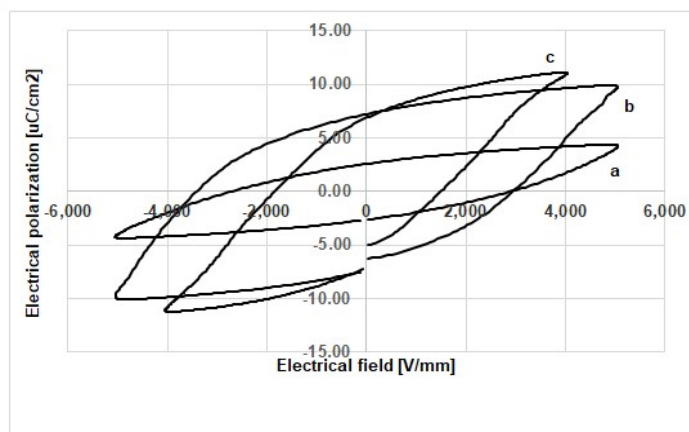


Fig.6 - Room temperature ferroelectric hysteresis loops of compositions (a) PZT-I1, (b) PZT-I2 and (c) PZT-I3 sintered for 2 h at 1200°C/ Curbele de histerezis la temperatura camerei pentru compozițiile (a) PZT-I1, (b) PZT-I2 și (c) PZT-I3 sinterizate timp de 2 ore la 1200°C.

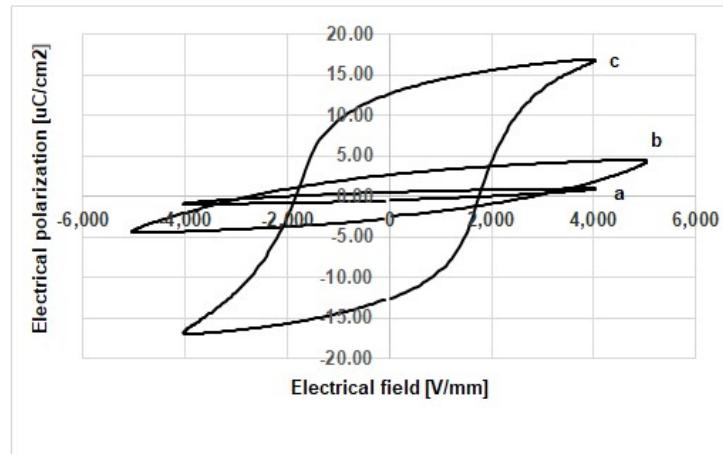


Fig.7 - Room temperature ferroelectric hysteresis loops of compositions (a) PZT-I1, (b) PZT-I2 and (c) PZT-I3 sintered for 2 h at 1250°C/ Curbele de histerezis la temperatura camerei pentru compozițiile (a) PZT-I1, (b) PZT-I2 și (c) PZT-I3 sinterizate timp de 2 ore la 1250°C.

The grain size effect is a very important factor in PZT ceramics because if the very large grain size is reduced the coercive field increases. The remnant polarization reflects the internal polarizability of the material. Therefore, high is the remnant polarization, high is the polarizability of the material.

The values obtained for the remaining polarization (P_r) and the coercive field (E_c) are in accordance with the results of the density and the structural characterization.

The hysteresis loops for the compositions PZT-I1, PZT-I2 and PZT-I3 sintered for 2 hours at 1200°C and 1250°C are symmetric and their forms are specific to ceramics with piezoelectric properties.

3.4. Dielectric and piezoelectric properties

At 1100°C and 1150°C the compositions PZT-I1, PZT-I2 and PZT-I3 could not be polarized due to the existing porosity. The porosity is the principle factor which contributes to the decrease the piezoelectric constants by reducing the polarization per unit volume, by reducing in piezoelectric charge constant. The maximum value of the piezoelectric charge constant is observed at PZT-I2 composition near MPB [37]. The co-existence of tetragonal and rhombohedral phases at MPB (phases that have nearly equivalent free energy) leads to increases in dielectric and piezoelectric properties.

For all the polarized compositions PZT-I1, PZT-I2 and PZT-I3, sintered at 1200°C and 1250°C the piezoelectric properties have been determined. The values of the dielectric losses ($\tan \delta$) increase as the sintering temperature increases. The microstructure of the composition is the determining factor for this variation.

A high degree of anisotropy is defined by an anisotropic ratio k_t/k_p (where k_t is thickness coupling factor and k_p is planar coupling factor) greater than 10 and involves low values of dielectric constant (ϵ_r) and a relatively high Curie temperature. A high value of anisotropic ratio indicates a greater degree of alignment of domains during the polarization treatment of the materials. The values obtained for k_t and k_p are dependent on the resonance frequency (f_r) and the antiresonance frequency (f_a) and are calculated with the formulas: $k_t^2 = \pi/2(f_r/f_a) \text{ctg} [\pi/2(f_r/f_a)]$, $k_p^2 = 2.51(f_a - f_r)/f_a$

The obtained values of the dielectric and piezoelectric properties for the compositions PZT-I1, PZT-I2 and PZT-I3 as a function of sintering temperature are shown in the Table 2.

4. Conclusions

In the present paper synthesis of ferroelectric materials prepared by a solid-state reaction technique, with general formula

Table 2
The dielectric and piezoelectric properties for the compositions PZT-I1, PZT-I2 and PZT-I3 as a function of sintering temperature/
Proprietățile dielectrice și piezoelectrice pentru compozițiile PZT-I1, PZT-I2 și PZT-I3 în funcție de temperatura de sinterizare

Sintering temperature [°C]	Sample ID	$\text{tg}\delta$	ϵ_r	f_r [MHz]	f_a [MHz]	k_t	k_p	k_t/k_p
1200	PZT I1	0.0096	405	1.3	1.4	9.0026	0.50	17.97
	PZT I2	0.0105	597	1.5	1.7	8.6663	0.54	15.95
	PZT I3	0.0104	594	1.4	1.7	8.2249	0.67	12.36
1250	PZT I1	0.012	325	1.4	1.6	8.6120	0.56	15.37
	PZT I2	0.013	461	1.3	1.5	8.5501	0.57	14.78
	PZT I3	0.017	725	1.4	1.5	9.0368	0.41	22.09

$0.98Pb(Zr_{1-x}Ti_x)O_3 - 0.02La(Fe^{3+}_{0.5}, Nb^{5+}_{0.5})O_3$, for different Zr^{4+}/Ti^{4+} ratios were investigated. Three different compositions for three different Zr^{4+}/Ti^{4+} ratios, modified with acceptor and donor dopants are selected: one is situated in tetragonal region (42/58), the second one is placed in MBP region (52/48) and the third one located in rhombohedral region (58/42). The density of the compositions increases as the sintering temperature increases. The coexistence of tetragonal and rhombohedral phases associated to high sintering temperatures improve the anisotropy. For the electromechanical coupling factor (k_p) the maximum value $k_p = 0.67$ was obtained for the composition sintered at 1200°C and with $x=0.58$.

Acknowledgment

The authors acknowledge the financial support of the project no. 133/23.09.2016, ID P_40_403, My SMIS code: 105568 co-funded of the European Regional Development Funds through the 2014-2020 Operational Competitiveness Program-Subcontract no.133 D1-ICPE for making possible the dissemination of these results.

REFERENCES

- [1] P. K. Panda, B. Sahoo, S. Raja, V. Shankar, Electromechanical and Dynamic Characterization of In-House-Fabricated Amplified Piezo Actuator, Smart Materials Research, 2012, 1–8
- [2] B. Sahoo, P. K. Panda, Fabrication of Simple and Ring-Type Piezo Actuators and Their Characterization, Smart Materials Research, 2012, 1–4
- [3] Eustaquio M.C., L. A. Velosa-Moncada, J. A. Del Angel-Arroyo, L. A. Aguilera-Cortés, Carlos A. Cerón-Álvarez, A.L. Herrera-May, Electromechanical Modeling of MEMS-Based Piezoelectric Energy Harvesting Devices for Applications in Domestic Washing Machines, Energies, 2020, **13(617)**, 1-16
- [4] C. Covaci, A. Gontean, Piezoelectric Energy Harvesting Solutions: A Review, Sensors, 2020, **20**, 3512, 1-37
- [5] B. Lin, V. Giurgiutiu, Pollock, P., B. Xu, J. Doane, Durability and Survivability of Piezoelectric Wafer Active Sensors on Metallic Structure, AIAA Journal, 2010, **48(3)**, 635–643
- [6] H.H. Kumar, C.M. Lonkar, K. Balasubramanian, Structure-Property Correlation and Harvesting Power from Vibrations of Aerospace Vehicles by Nanocrystalline $La-Pb(Ni_{1/3}Sb_{2/3})-PbZrTiO_3$ Ferroelectric Ceramics Synthesized by Mechanical Activation, Journal of the American Ceramic Society, 2016, **100(1)**, 215–223
- [7] R. Gupta, S. Verma, V. Singh, K.K. Bamzai, Preparation, Structural, Electrical, and Ferroelectric Properties of Lead Niobate–Lead Zirconate–Lead Titanate Ternary System, Journal of Ceramics, 2015, 1–12
- [8] B. Jaffe, W.R. Cook, H. Jaffe, Piezoelectric Ceramics, Academic Press, London, 1971, 317
- [9] B. Noheda, D.E. Cox, Bridging phases at the morphotropic boundaries of lead oxide solid solutions, Phase Transitions, 2006, **79(1-2)**, 5–20
- [10] M. Hinterstein, M. Hoelzel, J. Rouquette, J. Haines, J. Glaum, H. Kungl, M. Hoffman, Interplay of strain mechanisms in morphotropic piezoceramics, Acta Materialia, 2015, **94**, 319–327
- [11] C.M. Lonkar, D.K. Kharat, S. Prasad, B. Kandasubramanian, Synthesis, Characterization, and Development of PZT-Based Composition for Power Harvesting and Sensors Application, Handbook of Nanoceramic and Nanocomposite Coatings and Materials, 2015, 551–577
- [12] H.R. Nayan, Power Generation Using Piezoelectric Material, Journal of Material Science & Engineering, 2015, **04(03)**, 1-4
- [13] W. Qiu, H. H. Hng, Effects of dopants on the microstructure and properties of PZT ceramics. Materials Chemistry and Physics, 2002, **75(1-3)**, 151–156
- [14] D. J Singh, M. Ghita, M. Fornari, S. V. Halilov, Role of A-Site and B-Site Ions in Perovskite Ferroelectricity. Ferroelectrics, 2006, **338(1)**, 73–79
- [15] B. Sahoo, P. K. Panda, Dielectric, ferroelectric and piezoelectric properties of $(1-x)[Pb_{0.91}La_{0.09}(Zr_{0.60}Ti_{0.40})O_3]-x[Pb(Mg_{1/3}Nb_{2/3})O_3]$, $0 \leq x \leq 1$, Journal of Materials Science, 2007, **42(12)**, 4270–4275
- [16] T. Kamakshi, P. S. V. SubbaRao, Softening transitions in ferroelectric $Pb(Zr, Ti)O_3$ ceramics doped with neodymium oxide and lanthanum oxide, Journal of Applied Physics, 2014, **6(3)**, 50-55
- [17] M. Morozov, D. Damjanovic, N. Setter, The nonlinearity and subswitching hysteresis in hard and soft PZT, Journal of the European Ceramic Society, 2005, **25(12)**, 2483–2486
- [18] M.I. Morozov, D. Damjanovic, Hardening-softening transition in Fe-doped $Pb(Zr, Ti)O_3$ ceramics and evolution of the third harmonic of the polarization response, Journal of Applied Physics, 2008, **104(3)**, 034107-1- 034107-8
- [19] S. Sharma, R. Singh, T. C. Goel, S. Chandra, Synthesis, structural and electrical properties of La modified PZT system, Computational Materials Science, 2006, **37(1-2)**, 86–89
- [20] P.-H. Xiang, N. Zhong, X.-L. Dong, R.-H. Liang, H. Yang & C.-D. Feng, Fabrication and dielectric properties of lanthanum-modified lead zirconate titanate using coprecipitation powder coating, Materials Letters, 2004, **58(21)**, 2675–2678
- [21] M. Pereira, A.G. Peixoto, M.J.M. Gomes, Effect of Nb doping on the microstructural and electrical properties of the PZT ceramics, Journal of the European Ceramic Society, 2001, **21**, 10-11
- [22] J.E. Garcia, R. Pe'rez, A. Albareda, J.A. Eiras, Non-linear dielectric and piezoelectric response in undoped and Nb^{5+} or Fe^{3+} doped PZT ceramic system, Journal of the European Ceramic Society, 2007, **27**, 4029–4032
- [23] R. Rai, S. Sharma & R.N.P. Choudhary, Dielectric and piezoelectric studies of Fe doped PLZT ceramics, Materials Letters, 2005, **59(29-30)**, 3921–3925
- [24] A. Kumar, S.K. Mishra, Structural and dielectric properties of Nb and Fe co-doped PZT ceramic prepared by a semi-wet route, Advanced Materials Letters, 2014, **5(8)**, 479–484
- [25] A.I. Dumitru, G. Velciu, D. Patroi, J. Pinte, V. Marinescu, F. Clicinschi, L. Matekovits, I. Peter, Investigations on the doping effects on the properties of piezoelectric ceramics, Advanced Materials Research, 2020, **1158**, 105-114
- [26] T.M. Kamel, G. de With, Poling of hard ferroelectric PZT ceramics, Journal of the European Ceramic Society, 2008, **28(9)**, 1827–1838
- [27] A. Mirzaei, M. Bonyani, S. Torkian, Effect of Nb doping on sintering and dielectric properties of PZT ceramics, Processing and Application of Ceramics, 2016, **10(3)**, 175–182
- [28] M.-P. Zheng, Y. -D. Hou, F.-Y. Xie, J. Chen, M.-K. Zhu, H. Yan, Effect of valence state and incorporation site of cobalt dopants on the microstructure and electrical properties of 0.2PZN–0.8PZT ceramics, Acta Materialia, 2013, **61(5)**, 1489–1498
- [29] M.M.S. Pojucan, M.C.C. Santos, F.R. Pereira, M.A.S. Pinheiro & M.C. Andrade, Piezoelectric properties of pure and $(Nb^{5+} + Fe^{3+})$ doped PZT ceramics, Ceramics International, 2010, **36**, 1851–1855
- [30] A.I. Dumitru, G. Velciu, D. Patroi, J. Pinte, V. Marinescu, I. Peter, The influence of the sintering temperature on the properties of the $0.98Pb(Zr_{1-x}Ti_x)O_3 - 0.02La(Fe^{3+}_{0.5}, Nb^{5+}_{0.5})O_3$ ceramic systems, [Materials Science Forum](#), 2021, **1016**, 1134-1140
- [31] F. Kahoul, L. Hamzioui, Z. Necira, A. Boutarfaia, Effect of Sintering Temperature on the Electromechanical Properties of $(1-x)Pb(Zr_{1-x}Ti_x)O_3-xSm(Fe_{0.5}, Nb_{0.5})O_3$ Ceramics. Energy Procedia, 2013, **36**, 1050–1059

- [32] F. Kahoul, L. Hamzioui, A. Boutarfaia, The Influence of Zr/Ti Content on the Morphotropic Phase Boundary and on the Properties of PZT-SFN Piezoelectric Ceramics, *Energy Procedia*, 2014, **50**, 87–96
- [33] N. Vittayakorn, Rujijanagul, G. Tunkasiri, X.T. Tan, D. P. Cann, Perovskite phase formation and ferroelectric properties of the lead nickel niobate–lead zinc niobate–lead zirconate titanate ternary system, *Journal of Materials Research*, 2003, **18(12)**, 2882–2889
- [34] S. Takahashi, Effects of impurity doping in lead zirconate-titanate ceramics, *Ferroelectrics*, 1982, **41(1)**, 143–156
- [35] T. M. Kamel, G. With, Poling of hard ferroelectric PZT ceramics, *Journal of the European Ceramic Society*, 2008, **28(9)**, 1827–1838
- [36] P. Ketsuwan, A. Prasatkhetragarn, N. Triamnuk, C. C., Huang, A. Ngamjarrojana, S., Ananta, R. Yimnirun, Effects of Niobium Doping on Dielectric and Ferroelectric Properties of Chromium Modified Lead Zirconate Titanate Ceramics. *Ferroelectrics*, 2009, **380(1)**, 183–189
- [37] A. S. Karapuzha, N. K. James, Khanbareh, H. S., van der Zwaag, W. A. Groen, Structure, dielectric and piezoelectric properties of donor doped PZT ceramics across the phase diagram. *Ferroelectrics*, 2016, **504(1)**, 160–171
